



## Storage and Retrieval of THz-Bandwidth Single Photons Using a Room-Temperature Diamond Quantum Memory

Duncan G. England,<sup>1</sup> Kent A. G. Fisher,<sup>2</sup> Jean-Philippe W. MacLean,<sup>2</sup> Philip J. Bustard,<sup>1</sup>  
Rune Lausten,<sup>1</sup> Kevin J. Resch,<sup>2</sup> and Benjamin J. Sussman<sup>1,\*</sup>

<sup>1</sup>*National Research Council of Canada, 100 Sussex Drive, Ottawa, Ontario K1A 0R6, Canada*

<sup>2</sup>*Institute for Quantum Computing and Department of Physics and Astronomy, University of Waterloo,  
200 University Avenue West, Waterloo, Ontario N2L 3G1, Canada*

(Received 5 September 2014; published 5 February 2015)

We report the storage and retrieval of single photons, via a quantum memory, in the optical phonons of a room-temperature bulk diamond. The THz-bandwidth heralded photons are generated by spontaneous parametric down-conversion and mapped to phonons via a Raman transition, stored for a variable delay, and released on demand. The second-order correlation of the memory output is  $g^{(2)}(0) = 0.65 \pm 0.07$ , demonstrating a preservation of nonclassical photon statistics throughout storage and retrieval. The memory is low noise, high speed and broadly tunable; it therefore promises to be a versatile light-matter interface for local quantum processing applications.

DOI: [10.1103/PhysRevLett.114.053602](https://doi.org/10.1103/PhysRevLett.114.053602)

PACS numbers: 42.50.Ex, 03.67.Hk, 81.05.ug

Single photons are challenging to create, manipulate, and measure, yet are essential for a diverse range of quantum technologies, including cryptography [1], enhanced measurement [2], and information processing [3]. Quantum memories, which act as buffers for photonic states, are a key enabling component for these future technologies [4]. They allow repeat-until-success strategies to counteract the intrinsically probabilistic nature of quantum mechanics, thereby providing scalable quantum technologies. An ideal quantum memory would store a single photon, maintain the quantum state encoded in the photon, and release it, on demand, as a faithful recreation of the input. Efforts to implement optical quantum memories have used a number of platforms including single atoms in a cavity [5], ultracold atoms [6], atomic vapors [7], molecular gases [8], and rare-earth doped crystals [9].

The potential for quantum storage in optical memories is often investigated using laser pulses attenuated to the single-photon level [10]. However, the transition between storing weak coherent states and true single photons produces two significant obstacles. First, to achieve high efficiency, most memories must operate near resonance with a dipole transition, typically limiting storage bandwidths to  $\sim$ GHz or below [7,11]. Single-photon sources compatible with such devices require careful engineering to match the frequency and bandwidth of the photons to that of the memory [6,11–16]. Second, the intense read and write beams used to mediate storage and retrieval may introduce noise which obscures the quantum properties of the signal [17]. Where nonclassical memory operation has been demonstrated, laser-cooled [6,13,14] or cryogenic [11,12,15,16] substrates are often required to reduce noise.

In this Letter, we demonstrate the storage and retrieval of broadband single photons using a room-temperature

solid-state quantum memory. The THz-bandwidth heralded single photons are created by spontaneous parametric down-conversion (SPDC) and are stored, via an off-resonant Raman transition, in the optical phonon modes of a room-temperature bulk diamond. As the Raman interaction occurs far from any optical resonances, the memory can operate at a range of visible and near-infrared wavelengths. The bandwidth of the memory is limited only by the 40 THz splitting between the ground and storage states [18]. This broad bandwidth and large tuning range makes the memory compatible with ultrafast SPDC photon sources [19]. Furthermore, the memory exhibits a quantum-level noise floor, even at room temperature [20].

The memory utilized a high-purity, low-birefringence synthetic diamond manufactured by Element Six Ltd. The diamond, which is 2.3 mm thick, was grown by chemical vapor deposition and is cut along the  $\langle 100 \rangle$  face of the diamond lattice. The relevant energy levels can be described by a  $\Lambda$ -level system consisting of the crystal ground state  $|0\rangle$ , an optical phonon acting as the storage state  $|1\rangle$ , and an off-resonant intermediate state  $|2\rangle$  representing the conduction band. Single photons are stored to, and retrieved from, the optical phonon by strong *write* and *read* pulses via an off-resonant Raman interaction [7,21]. The photons and read-write pulses are in two-photon resonance with the optical phonon energy [see Fig. 1(b)]. In the  $\langle 100 \rangle$  configuration, the Raman interaction couples fields of orthogonal polarization [22] such that the *H*-polarized input photons are stored by a *V*-polarized write pulse and *V*-polarized output photons are retrieved using a *H*-polarized read pulse. Because of these selection rules, the memory stores only a single polarization mode and not a polarization encoded qubit. Polarization storage in such memories can be achieved by using spatial multiplexing techniques [6].

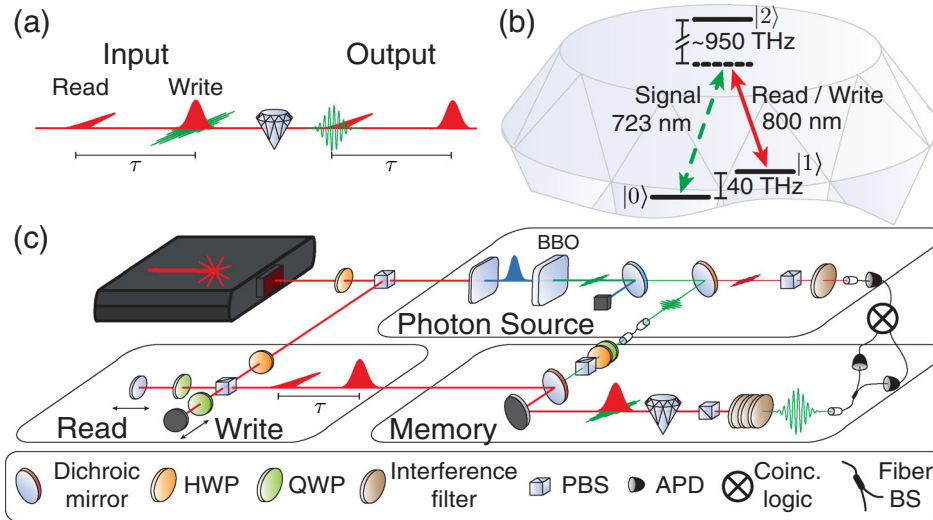


FIG. 1 (color online). Experimental concept, energy level diagram, and setup. (a) The memory protocol. A horizontally ( $H$ ) polarized single photon (green, 723 nm) is written into the quantum memory with a vertically ( $V$ ) polarized write pulse (red, 800 nm). After a delay  $\tau$ , an  $H$ -polarized read pulse recalls a  $V$ -polarized photon. (b) Energy levels in the memory. The ground state  $|0\rangle$  and the storage state  $|1\rangle$  correspond to the crystal ground state and an optical phonon, respectively. The signal photon and the read-write pulses are in two-photon resonance with the optical phonon (40 THz) and are far detuned from the conduction band  $|2\rangle$ . (c) The experimental setup. The laser output is split to pump the photon source and to produce the orthogonally polarized read and write beams. The photons are produced in pairs with one (signal) at 723 nm and the other (herald) at 895 nm. The signal photon is stored in, and recalled from, the quantum memory. The herald and signal photons are detected using APDs and correlations between them are measured using a coincidence logic unit.

The high carrier frequency of the optical phonon (40 THz [18]) and a large detuning from the conduction band ( $\sim 950$  THz) are the key features allowing storage of THz-bandwidth photons. These features also provide an intrinsically low noise floor: the large detuning from optical resonance eliminates fluorescence noise, and the high energy of the optical phonon results in low thermal phonon population at room temperature. Four-wave mixing noise, which is a pervasive problem in many  $\Lambda$ -level systems [17,23], is suppressed in diamond due to the large splitting and the high optical dispersion [20]. Following excitation, the optical phonons decay into a pair of acoustic phonons with a characteristic time scale of 3.5 ps [24], which sets the storage lifetime of the memory. The advantage of the rapid acoustic decay is that it returns the crystal lattice to the ground state, resetting the memory such that it is ready to store the next photon. This subnanosecond reset time permits GHz repetition rates in the diamond phonon system.

The high bandwidth and rapid reset time of our memory may benefit local quantum processing applications such as quantum frequency conversion [25], memory-enhanced optical nonlinearities [26], or programmable linear-optical components [27]. However, the lifetime is too short for quantum communication protocols [28]. The diamond memory is complementary to existing atomic [6] or rare-earth-doped [9] quantum memories: the long storage times of the latter benefiting long-distance quantum communication and the high bandwidth of the former providing advantages for small-scale quantum processing. To leverage the full bandwidth of this memory, we require multiple operational

time bins during storage. This could be achieved by creating multiple time-delayed replicas of an 80 MHz laser pulse train to generate bursts of pulses separated by  $\ll 1$  ps [29]; these bursts could be used to pump a SPDC source.

The master laser for the experiment is a mode-locked Ti:sapphire laser producing pulses of 190 fs duration at a repetition rate of 80 MHz, a central wavelength of 800 nm, and a pulse energy of 28 nJ. The laser beam is split between the photon source and the memory with 12.5 nJ used to generate the orthogonally polarized read and write pulses [read-write panel, Fig. 1(c)]. The remaining energy for the photon source is frequency doubled in a 1 mm  $\beta$ -barium borate (BBO) crystal to produce pulses at 400 nm (pulse energy 2.4 nJ). In a second 1 mm BBO crystal, angle tuned to phase match type I nondegenerate SPDC, the pump field at 400 nm produces horizontally polarized photon pairs at 723 nm (signal) and 895 nm (herald). The photon pairs are emitted collinearly from the BBO and, after the remaining 400 nm pump light has been removed by interference filters, the signal and herald photons are spatially separated by an 801 nm long-pass dichroic mirror. The herald photons pass through a polarizing beam splitter (PBS) and a 5 nm bandwidth interference filter before being coupled into a single-mode fiber and detected on an avalanche photodiode (APD). The signal photons are coupled into a 7 cm long single-mode fiber for spatial filtering before being directed to the memory.

The horizontally polarized signal photon is spatially and temporally overlapped on a dichroic mirror with the vertically polarized write pulse and focused into the diamond for storage by a 6 cm focal length achromatic lens. After a time

delay  $\tau$ , the horizontally polarized read pulse arrives at the memory and the photon is reemitted, this time with vertical polarization. We can thus distinguish between the input and the output states of the memory by their polarization [Fig. 1(a)]. Following the memory, the signal photons are spectrally filtered from the read-write pulses using interference filters [30] and coupled into a single-mode fiber. By rotating the polarization basis we collect either the memory output or the unabsorbed memory input [memory panel, Fig. 1(c)]. The photons are detected by an APD and correlations in photon detection events are measured using coincidence counting logic.

Storage of the signal photons is demonstrated by scanning the delay of the write pulse with respect to the signal photon. With 12.5 nJ in the write pulse, a 20% reduction in signal-herald coincidences at zero delay indicates that signal photons are being written to the memory (inset, Fig. 2). The full width at half maximum of the absorption profile is  $w_a = 326$  fs. Deconvolving this width with that of the write pulse ( $w_w = 190$  fs) using the expression  $w_a^2 = w_w^2 + w_\gamma^2$  returns an estimated photon duration of  $w_\gamma = 260$  fs, assuming transform limited pulses with Gaussian spectra.

Readout of the signal photons is observed by rotating the polarization filter to measure the vertically polarized output of the memory. With 6.25 nJ in each pulse, we scan the delay between the write and read pulses; the sharp step in signal-herald coincidences at zero delay indicates that signal photons are being retrieved from the memory

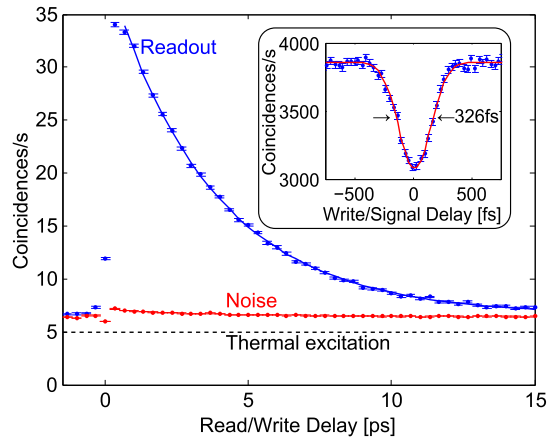


FIG. 2 (color online). Measured coincidences between the signal and herald photons as a function of read-write delay (blue bars). An exponential decay of half-life 3.5 ps (solid blue fit) is characteristic of the optical phonon lifetime. The background noise (red bars) shows a SNR of 3.8:1 for single photon retrieval. The estimated noise due to thermal phonon population is shown by the dotted line. *Inset*: Transmission through the diamond in the presence of the write pulse, showing memory absorption. The profile width of 326 fs (solid red fit) indicates the large bandwidth of the photons stored in the memory. All error bars are from poissonian counting statistics. Signal and herald detection events are defined as coincident if the time delay between them falls within a 1 ns window.

(Fig. 2). The exponential decay in read efficiency has a half-life of 3.5 ps, which is characteristic of the optical phonon lifetime [24]. We have therefore demonstrated that the memory stores a single photon for over 13 times its duration. The maximum total memory efficiency is  $\eta_t = 0.9\%$  and the write efficiency is  $\eta_w = 9\%$ , from which we extract a read efficiency of  $\eta_r = \eta_w/\eta_t = 10\%$ . The memory efficiency was limited by available laser power but could be improved by using high-energy read-write pulses, as has been demonstrated in other Raman memories [8], or by exploiting enhanced coupling in a waveguide structure [31].

By blocking the input signal photons we can measure the background noise of the memory (see Fig. 2): the maximum signal-to-noise ratio (SNR) is 3.8:1; it is important to note that this is a raw measurement and no background subtraction has been performed. This noise has two origins: spontaneous anti-Stokes scattering from thermally excited phonons and spontaneous four-wave mixing (FWM). The FWM noise process is intrinsic to the memory and cannot be completely eliminated; however, in a dispersive material such as diamond it is strongly suppressed due to phase-matching conditions [20]. From Boltzmann statistics we calculate that around 5 coincidence counts per second can be attributed to thermal noise (the dashed line in Fig. 2), we note that the thermal noise could be reduced by an order of magnitude by cooling the diamond to  $-60^\circ\text{C}$ , for example by using a Peltier element. The photon heralding efficiency at the memory is 16%, meaning that a single photon is present at the memory in only 16% of the heralded experiments; despite this, we still observe a high contrast between signal and noise. At  $-60^\circ\text{C}$ , with an ideal heralding efficiency, the SNR in this memory could be 70:1.

Correlations between the memory output and the herald photon can be seen in their coincidence statistics, as shown in Fig. 3. The coincidence rate as a function of the electronic delay between the memory output and the herald photon shows periodic peaks due to accidental coincidences between the memory noise and the herald photon; the time period of these peaks is 12.5 ns, corresponding to the repetition period of the laser oscillator. The largest peak, at zero delay, indicates a retrieval of signal photons which have been written to the memory. These coincidence rates exceed the accidental rate by a factor of 5, a clear indication that the nonclassical correlations between herald and signal are maintained during storage and retrieval from the quantum memory.

A stringent test for nonclassical photon statistics is to measure the second-order correlation function  $g^{(2)}(0)$  [32]. Using the Hanbury Brown–Twiss configuration [33], the input light field is partitioned between two detectors using a 50:50 fiber beam splitter, as shown in Fig. 1(c). The triggered  $g^{(2)}(0)$  function of the heralded SPDC source is calculated as [34]

$$g^{(2)}(0) = \frac{N_{h,1,2}N_h}{N_{h,1}N_{h,2}}, \quad (1)$$

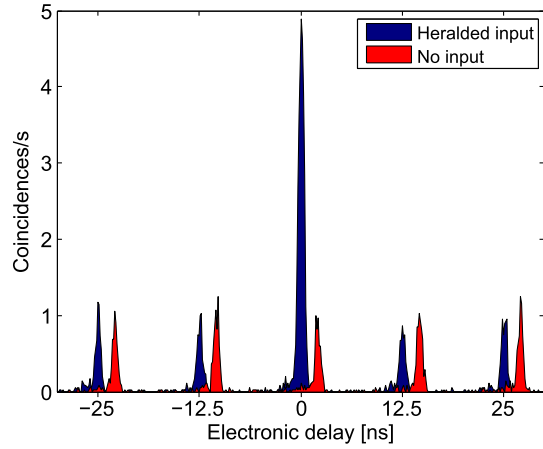


FIG. 3 (color online). Detection coincidences between the herald photon and the signal photon retrieved from the memory as a function of electronic delay (blue). A peak of 5 times the accidental rate at zero delay demonstrates strong correlations between the herald and signal photons after readout from the memory. The memory noise (red, offset by 2 ns for clarity) shows no increase at zero delay. Signal and herald detection events are defined as coincident if the time delay between them falls within a 156 ps window. The width of the peaks is due to the timing jitter ( $\sim 500$  ps) of the APDs.

where  $N_h$  is the number of herald photons detected in a given time window,  $N_{h,1}$  ( $N_{h,2}$ ) is the number of twofold coincident detections between the herald and output port 1 (2) of the beam splitter and  $N_{h,1,2}$  is the number of threefold coincidences between the herald and both ports of the beam splitter. A correlation function of  $g^{(2)}(0) < 1$  is a direct measure of sub-Poissonian statistics which cannot be explained classically and is evidence of single photons.

At the memory input, we measure  $g_{\text{in}}^{(2)}(0) = 0.04 \pm 0.01$ ; after the memory the correlation function  $g_{\text{out}}^{(2)}(0)$

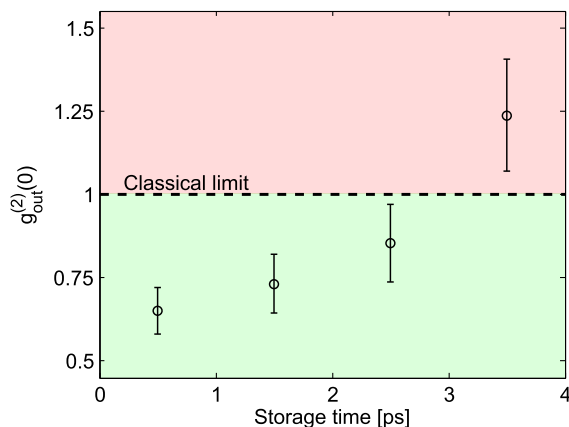


FIG. 4 (color online). The heralded second-order correlation function of the memory output as a function of storage time. Values below the classical limit of  $g_{\text{out}}^{(2)}(0) = 1$  demonstrate the quantum characteristics of the output field. Nonclassical statistics are observed for storage times up to  $\sim 3$  ps. Error bars are from Poissonian counting statistics.

depends on the storage time, as shown in Fig. 4. When the storage time is 0.5 ps, we measure  $g_{\text{out}}^{(2)}(0) = 0.65 \pm 0.07$ , 5 standard deviations below the classical limit of 1. The measured  $g_{\text{out}}^{(2)}(0)$  function increases with increasing storage time, as the noise comprises a larger fraction of the measured counts; however, the memory output maintains nonclassical statistics for  $> 2.5$  ps. A  $g_{\text{out}}^{(2)}(0)$  correlation of 0.65 confirms nonclassicality, but the storage and readout has introduced noise, thereby degrading the correlation measured directly from the source,  $g_{\text{in}}^{(2)}(0)$ . For completeness, we point out that a  $g_{\text{out}}^{(2)}(0) > 0.5$  cannot distinguish between a state comprised of single photons mixed with thermal noise and a different nonclassical state comprised entirely of  $n = 2$  and larger Fock states. However the latter state is unlikely given the physics of the system.

In conclusion, we have demonstrated a THz-bandwidth quantum memory for light using the optical phonon modes of a room-temperature diamond. The unique features of the memory enable storage of single photons produced by ultrafast spontaneous parametric down-conversion—the most widespread source of single and entangled photons. The heralded second-order correlation function of the memory output was  $g_{\text{out}}^{(2)}(0) = 0.65 \pm 0.07$ , which is 5 standard deviations below the classical limit. This result confirms the quantum nature of our memory by mapping a single photon to and from a single phonon maintaining nonclassical photon statistics. The device requires no cooling or optical preparation before storage and is a few millimeters in size; diamond is therefore a robust, convenient, and high-speed test bed system in which to evaluate operational memory parameters, study the effects of noise, and develop quantum protocols.

The authors thank Matthew Markham and Alastair Stacey of Element Six Ltd. for the diamond sample. They also thank Paul Hockett and Josh Nunn for useful discussions, and John Donohue for writing data acquisition software. Doug Moffatt and Denis Guay provided invaluable technical assistance. This work was supported by the Natural Sciences and Engineering Research Council of Canada, Canada Research Chairs, the Canada Foundation for Innovation, Ontario Centres of Excellence, and the Ontario Ministry of Research and Innovation Early Researcher Award.

\*ben.sussman@nrc.ca

- [1] C. H. Bennett and G. Brassard, Quantum cryptography: Public key distribution and coin tossing, in *Proceedings of IEEE International Conference on Computers, Systems and Signal Processing, Bangalore, India, 1984* (IEEE, New York, 1984).
- [2] V. Giovannetti, S. Lloyd, and L. Maccone, Quantum-enhanced measurements: Beating the standard quantum limit, *Science* **306**, 1330 (2004).

- [3] E. Knill, R. Laflamme, and G. J. Milburn, A scheme for efficient quantum computation with linear optics, *Nature (London)* **409**, 46 (2001).
- [4] F. Bussières, N. Sangouard, M. Afzelius, H. de Riedmatten, C. Simon, and W. Tittel, Prospective applications of optical quantum memories, *J. Mod. Opt.* **60**, 1519 (2013).
- [5] H. P. Specht, C. Nolleke, A. Reiserer, M. Uphoff, E. Figueroa, S. Ritter, and G. Rempe, A single-atom quantum memory, *Nature (London)* **473**, 190 (2011).
- [6] K. S. Choi, H. Deng, J. Laurat, and H. J. Kimble, Mapping photonic entanglement into and out of a quantum memory, *Nature (London)* **452**, 67 (2008).
- [7] K. F. Reim, J. Nunn, V. O. Lorenz, B. J. Sussman, K. C. Lee, N. K. Langford, D. Jaksch, and I. A. Walmsley, Towards high-speed optical quantum memories, *Nat. Photonics* **4**, 218 (2010).
- [8] P. J. Bustard, R. Lausten, D. G. England, and B. J. Sussman, Toward Quantum Processing in Molecules: A THz-Bandwidth Coherent Memory for Light, *Phys. Rev. Lett.* **111**, 083901 (2013).
- [9] M. P. Hedges, J. J. Longdell, Y. Li, and M. J. Sellars, Efficient quantum memory for light, *Nature (London)* **465**, 1052 (2010).
- [10] H. de Riedmatten, M. Afzelius, M. U. Staudt, C. Simon, and N. Gisin, A solid-state light-matter interface at the single-photon level, *Nature (London)* **456**, 773 (2008).
- [11] E. Saglamyurek, N. Sinclair, J. Jin, J. A. Slater, D. Oblak, F. Bussières, M. George, R. Ricken, W. Sohler, and W. Tittel, Broadband waveguide quantum memory for entangled photons, *Nature (London)* **469**, 512 (2011).
- [12] E. Saglamyurek, J. Jin, V. B. Verma, M. D. Shaw, F. Marsili, S. W. Nam, D. Oblak, and W. Tittel, Quantum storage of entangled telecom-wavelength photons in an erbium-doped optical fibre, *Nat. Photonics* **9**, 83 (2015).
- [13] T. Chanelière, D. N. Matsukevich, S. D. Jenkins, S.-Y. Lan, T. A. B. Kennedy, and A. Kuzmich, Storage and retrieval of single photons transmitted between remote quantum memories, *Nature (London)* **438**, 833 (2005).
- [14] H. Zhang, X.-M. Jin, J. Yang, H.-N. Dai, S.-J. Yang, T.-M. Zhao, J. Rui, Y. He, X. Jiang, F. Yang, G.-S. Pan, Z.-S. Yuan, Y. Deng, Z.-B. Chen, X.-H. Bao, S. Chen, B. Zhao, and J.-W. Pan, Preparation and storage of frequency-uncorrelated entangled photons from cavity-enhanced spontaneous parametric downconversion, *Nat. Photonics* **5**, 628 (2011).
- [15] C. Clausen, I. Usmani, F. Bussières, N. Sangouard, M. Afzelius, H. de Riedmatten, and N. Gisin, Quantum storage of photonic entanglement in a crystal, *Nature (London)* **469**, 508 (2011).
- [16] D. Rieländer, K. Kutluer, P. M. Ledingham, M. Gündoğan, J. Fekete, M. Mazzer, and H. de Riedmatten, Quantum Storage of Heralded Single Photons in a Praseodymium-Doped Crystal, *Phys. Rev. Lett.* **112**, 040504 (2014).
- [17] P. S. Michelberger, T. F. M. Champion, M. R. Sprague, K. T. Kaczmarek, M. Barbieri, X. M. Jin, D. G. England, W. S. Kolthammer, D. J. Saunders, J. Nunn, and I. A. Walmsley, Interfacing GHz-bandwidth heralded single photons with a room-temperature Raman quantum memory, *arXiv:1405.1470*.
- [18] S. A. Solin and A. K. Ramdas, Raman spectrum of diamond, *Phys. Rev. B* **1**, 1687 (1970).
- [19] P. J. Mosley, J. S. Lundeen, B. J. Smith, P. Wasylczyk, A. B. U'Ren, C. Silberhorn, and I. A. Walmsley, Heralded Generation of Ultrafast Single Photons in Pure Quantum States, *Phys. Rev. Lett.* **100**, 133601 (2008).
- [20] D. G. England, P. J. Bustard, J. Nunn, R. Lausten, and B. J. Sussman, From Photons to Phonons and Back: A THz Optical Memory in Diamond, *Phys. Rev. Lett.* **111**, 243601 (2013).
- [21] J. Nunn, I. A. Walmsley, M. G. Raymer, K. Surmacz, F. C. Waldermann, Z. Wang, and D. Jaksch, Mapping broadband single-photon wave packets into an atomic memory, *Phys. Rev. A* **75**, 011401 (2007).
- [22] W. Hayes and R. Loudon, *Scattering of Light by Crystals* (Dover Science Books, New York, 1978).
- [23] N. Lauk, C. O'Brien, and M. Fleischhauer, Fidelity of photon propagation in electromagnetically induced transparency in the presence of four-wave mixing, *Phys. Rev. A* **88**, 013823 (2013).
- [24] K. C. Lee, B. J. Sussman, M. R. Sprague, P. Michelberger, K. F. Reim, J. Nunn, N. K. Langford, P. J. Bustard, D. Jaksch, and I. A. Walmsley, Macroscopic non-classical states and terahertz quantum processing in room-temperature diamond, *Nat. Photonics* **6**, 41 (2012).
- [25] H. J. McGuinness, M. G. Raymer, C. J. McKinstrie, and S. Radic, Quantum Frequency Translation of Single-Photon States in a Photonic Crystal Fiber, *Phys. Rev. Lett.* **105**, 093604 (2010).
- [26] M. Hosseini, S. Rebic, B. M. Sparkes, J. Twamley, B. C. Buchler, and P. K. Lam, Memory-enhanced noiseless cross-phase modulation, *Light Sci. Appl.* **1**, e40 (2012).
- [27] K. F. Reim, J. Nunn, X.-M. Jin, P. S. Michelberger, T. F. M. Champion, D. G. England, K. C. Lee, W. S. Kolthammer, N. K. Langford, and I. A. Walmsley, Multipulse Addressing of a Raman Quantum Memory: Configurable Beam Splitting and Efficient Readout, *Phys. Rev. Lett.* **108**, 263602 (2012).
- [28] C. Simon, H. de Riedmatten, M. Afzelius, N. Sangouard, H. Zbinden, and N. Gisin, Quantum Repeaters with Photon Pair Sources and Multimode Memories, *Phys. Rev. Lett.* **98**, 190503 (2007).
- [29] A. M. Weiner and D. E. Leaird, Generation of terahertz-rate trains of femtosecond pulses by phase-only filtering, *Opt. Lett.* **15**, 51 (1990).
- [30] The read-write pulses were removed using four angle-tuned notch filters (Semrock NF03-808E-25). The single photons were spectrally isolated from other noise photons using a 723 nm bandpass filter (Foreal Inc., 5 nm bandwidth).
- [31] M. P. Hiscocks, K. Ganesan, B. C. Gibson, S. T. Huntington, F. Ladouceur, and S. Praver, Diamond waveguides fabricated by reactive ion etching, *Opt. Express* **16**, 19512 (2008).
- [32] R. J. Glauber, The quantum theory of optical coherence, *Phys. Rev.* **130**, 2529 (1963).
- [33] R. Hanbury Brown and R. Q. Twiss, Correlation between photons in two coherent beams of light, *Nature (London)* **177**, 27 (1956).
- [34] P. Grangier, G. Roger, and A. Aspect, Experimental evidence for a photon anticorrelation effect on a beam splitter: A new light on single-photon interferences, *Europhys. Lett.* **1**, 173 (1986).